The submitted manuscript has been authored by a contractor of the U. S. Government under contract No. W-31-109-ENG-38. Accordingly, the U. S. Government retains a nonexclusive, royalty-free license to publish or reproduce the published form of this contribution, or allow others to do so, for U. S. Government purposes.

CONF-9606278--1
ANL/HEP/CP--96-62
RECEIVED
SEP 19 1996
OSTI

ANL-HEP-CP-96-62

Manifestations of the axial anomaly in finite temperature QCD

J.B. Kogut[a*], J.-F. Lagaë[b†] and D.K. Sinclair[b†]

[a]Department of Physics, University of Illinois, 1110 West Green Street, Urbana IL 61801, USA

[b]HEP Division, Argonne National Laboratory, 9700 South Cass Avenue, Argonne IL 60439, USA

We compute the flavor singlet meson correlators and screening masses in quenched and $N_f = 2$ QCD at $N_t = 8$. The consequences of our results for the realization of the $U_A(1)$ symmetry at finite T are discussed and an interpretation of our measurements in terms of the behaviour of the low lying fermionic modes is proposed.

Although the QCD chiral phase transition has been studied for many years, relatively little is known so far about the realization of the axial $U(1)$ symmetry in finite temperature QCD. The limiting cases are understood however: at very high temperature the $U_A(1)$ symmetry can be considered as "effectively restored" (since the effects associated with the axial anomaly are small in a dilute gas of instantons) whereas at zero temperature a sizeable explicit breaking of the $U_A(1)$ symmetry is essential to our understanding of meson spectroscopy. The question therefore arises as to how the transition between these two regimes is realized and how this relates to the restoration of the $SU(N_f)$ chiral symmetry. In order to investigate this problem, we have computed mesonic screening correlators at various temperatures above and below the phase transition. Considering 2 flavors of valence quarks, we do this in 4 channels corresponding to the $\vec{\pi}$, σ, $\vec{\delta}$ and η'. Chiral symmetry restoration would then induce degeneracies represented by the following grouping of states: $(\vec{\pi}, \sigma)$ and $(\vec{\delta}, \eta')$, while $U_A(1)$ restoration would imply: (σ, η') and $(\vec{\pi}, \vec{\delta})$.

Our lattice computations are done using staggered quarks. The operators representing the $\vec{\pi}$, σ, $\vec{\delta}$ and η' are respectively $\gamma_5 \otimes \xi_5$, $I \otimes I$, $I \otimes \xi_5$ and $\gamma_5 \otimes I$. The first two being local operators and the last two 4-link operators. In order to minimize the effect of flavor symmetry breaking (which can be substantial at the values of β currently used) it is desirable to limit comparisons to one of the two categories. This strategy allows a study of the $\vec{\pi}, \sigma, \vec{\delta}$ system with minimal lattice artifacts if one replaces the $\vec{\delta}$ correlator by the connected part of the σ correlator (σ_{conn}). This being said, the computations involving the η' operator are also quite important in exposing the underlying physics, since (through the Atyah-Singer index theorem) $\gamma_5 \otimes I$ serves as an indicator of topological activity in the QCD vacuum. All our correlators (connected and disconnected) were computed using a $U(1)$ noisy estimator following the techniques used by Kilcup et al. in zero temperature QCD [1]. In addition to this and in order to help in the interpretation of our results we also computed the low lying spectrum of the Dirac operator (in practice the lowest 8 eigenvalues and associated eigenvectors) on each of our configurations. This was done using the conjugate gradient algorithm investigated by Kalkreuter and Simma [2]. As we will show later, some of the correlators are entirely saturated by the few lowest fermionic modes, allowing further insight into the dynamics of finite temperature QCD.

All our computations were done on the CRAY C-90 at NERSC on lattices of size $16^3 \times 8$. We have gathered results both for quenched and 2 flavor QCD. A single value of the quark mass has been studied so far: $ma = 0.02$ for the quenched case and $ma = 0.00625$ in 2 flavor QCD. In the later case, we use configurations generated by the HTMCGC collaboration [3]. The quenched computations are done at $\beta = 5.8, 5.9, 6.0, 6.1$ and 6.2 where we have respectively analyzed 100, 100, 100, 170 and 170 configurations. Similar num-

*Supported in part by NSF grant NSF-PHY92-00148.
†Supported by DOE contract W-31-109-ENG-38.

DISTRIBUTION OF THIS DOCUMENT IS UNLIMITED

MASTER

DISCLAIMER

Portions of this document may be illegible in electronic image products. Images are produced from the best available original document.

bers for the 2 flavor case are $\beta = 5.45$ [160], 5.475 [240], 5.5 [160], 5.525 [160] and 5.55 [80]. The position of the crossover is found to be slightly higher than $\beta = 6.0$ in the quenched case and slightly higher than $\beta = 5.475$ in two flavor QCD. In figure 1, we plot our results for the $\vec{\pi}, \sigma$ and $\vec{\delta}$ screening lengths in 2 flavor QCD as a function of β. The key feature of this plot is that the σ becomes light close to the transition while the $\vec{\delta}$ remains heavy. This is in agreement with the observation that the peak in the scalar susceptibility originates in the disconnected part of the correlator [4]. Above the phase transition, the $U_A(1)$

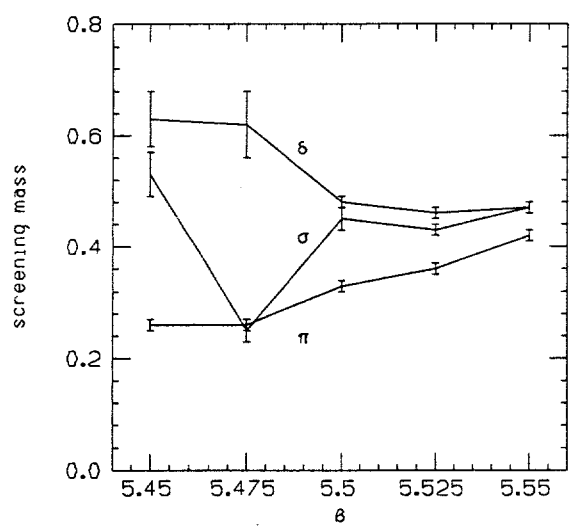

Figure 1. Screening masses in two flavor QCD

symmetry breaking ($m_{\vec{\delta}} - m_{\vec{\pi}}$) appears to be of the same order as the explicit chiral symmetry breaking ($m_\sigma - m_{\vec{\pi}}$) at our current value of the quark mass ($ma = 0.00625$). A careful extrapolation to the chiral limit will therefore be necessary in order to precisely sort out the situation in this region. This is currently being attempted by other groups [5–7], although they only compute the integrated correlators (susceptibilities) instead of the full correlators as we do here. Using the data already available at this stage, however, it is tempting to speculate that the $U_A(1)$ symmetry is not restored within the critical region. Using the HTMCGC data for the $\vec{\delta}$ correlator at $ma = 0.0125$ [8] together with ours, it appears that $m_{\vec{\delta}}$ extrapolates to a non-zero number at all values of β. Assuming a second order transition however, m_σ (and $m_{\vec{\pi}}$) will become very light close to the transition. Hence it appears that while $SU(2)_L \times SU(2)_R$ is being restored, $U_A(1)$ breaking is still present and only disappears at higher temperatures.

As mentioned earlier we have also computed the lowest 8 eigenvalues and associated eigenvectors on each of our configurations. Interestingly, we find that a spectral expansion of the quark propagator truncated to these low lying modes already captures a significant part of the physics. At or above the transition, for example, the pseudoscalar disconnected correlator is completely saturated by these low lying modes (similar computations below the phase transition are currently in progress). This suggests that a rather detailed description of the dynamics associated with the phase transition can be obtained. In the continuum, we expect to find two kinds of low lying modes: exact zero modes (which must appear in number consistent with the index theorem: $n_+ - n_- = N_f Q_{top}$) and near zero modes (with no a priori connection to topology). Modes from the first category satisfy $r = 1$ with $r = | < n|\gamma_5|n > |$, whereas those from the second necessarily have $r = 0$. On the lattice however, these results are not reproduced exactly. Topological zero modes are shifted away from zero and averages of the lattice Γ_5 operator can differ significantly from the numbers given above [9]. By combining the two pieces of information (λ and r), it is however often possible to decide on the topological or non-topological character of a given mode. This can be done for example by drawing a plot of $| < n|\gamma_5|n > |$ versus $|\lambda_n|$. Diagrams of this kind were considered by Hands and Teper in zero temperature QCD [10]. Here, we will focus our attention on the high temperature regime and leave the discussion of the transition region for a longer presentation [11]. Our results for quenched QCD at $\beta = 6.2$ are gathered on figure 2. In order to check the consistency of our results with other methods, we also cooled the configurations and

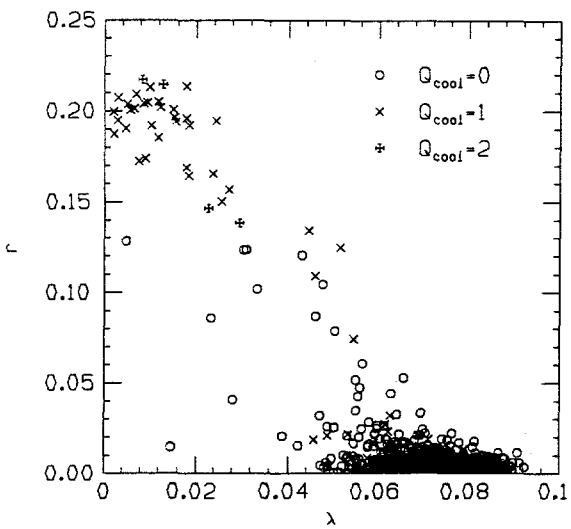

Figure 2. (r, λ) diagram in quenched QCD at $\beta = 6.2$

assigned them an *integer* topological charge Q_{cool}. Results obtained on configurations with different Q_{cool} are represented by different symbols on figure 2 (see insert). The results behave according to expectations; in particular, there is a strong correlation between large r and small eigenvalues and topological zero mode candidates can easily be identified. Note that they have a value of r around 0.20 only instead of 1 (This is to be expected since Γ_5 being a 4-link operator picks up a large correction factor already in the mean-field approximation). By looking at these results configuration by configuration, one can check that the number of topological (zero) modes is exactly $4Q_{cool}$ (the 4 being associated with the 4 flavor of staggered fermions). The unique configuration with topological charge 2 in our sample, for example, gives us 4 low modes in figure 2 (the existence of 4 other modes with opposite eigenvalue being guaranteed by the symmetries of the lattice Dirac operator). Finally, figure 2 also shows 4 modes with low eigenvalues but small r. They all come from one given configuration with topological charge 0. An analysis of the local values of $< n|\Gamma_5(x)|n >$ reveals that this configuration contains an $I - \bar{I}$ pair and that the 4 fermionic modes are delocalized over the 2 topological objects. In the continuum, this would give rise to a small but non-zero eigenvalue. On the lattice, the 4 copies have different eigenvalues and different amount of delocalization because of flavor symmetry breaking. In conclusion of this analysis, we see that in quenched QCD at $\beta = 6.2$ the disconnected pseudoscalar correlator is dominated by the contribution from topological zero modes (most of them with topological charge ± 1). As the temperature is lowered, the number of small but non-exact zero modes increases and the region close to the origin fills up in the (λ, r) diagram. Finally, we should mention that the shift in the eigenvalue of topological modes (extending at least to the interval [-0.02,0.02] in figure 2) implies that we should be very careful in attempting an extrapolation to the chiral limit. Using masses lower than 0.02 for example would lead to a significant underestimate of the quantities measured. It is also important to realize that the shift of topological modes is an ultraviolet effect (which could for example be corrected by the use of an improved or perfect action) and is therefore completely different from the depletion of eigenvalues of order $1/V$ commonly observed in measurements of $< \bar{\psi}\psi >$ (which is a finite size effect).

REFERENCES

1. G.Kilcup, J.Grandy and L. Venkataraman, Nucl.Phys.B(PS), **47** (1996) 358
2. T.Kalkreuter and H.Simma, Comput. Phys. Commun. **93**, 33 (1996)
3. S. Gottlieb et al., in preparation
4. F.Karsch and E.Laermann, Phys. Rev. D **50** (1994) 6954
5. S.Chandrasekharan and N.Christ, Nucl.Phys. B(PS)**47** (1996)527; N.Christ, this conference
6. T.Blum and C.DeTar, this conference
7. G.Boyd et al., hep-lat/9607046 (1996)
8. S.Gottlieb et al., Phys.Rev.D**47**,3619(1993)
9. J.C.Vink, Phys. Lett. **210**B (1988) 211
10. S.J.Hands and M.Teper, Nucl. Phys. **B347**, 819 (1990)
11. J.B.Kogut, J.-F.Lagaë and D.K.Sinclair, in preparation

DISCLAIMER

This report was prepared as an account of work sponsored by an agency of the United States Government. Neither the United States Government nor any agency thereof, nor any of their employees, makes any warranty, express or implied, or assumes any legal liability or responsibility for the accuracy, completeness, or usefulness of any information, apparatus, product, or process disclosed, or represents that its use would not infringe privately owned rights. Reference herein to any specific commercial product, process, or service by trade name, trademark, manufacturer, or otherwise does not necessarily constitute or imply its endorsement, recommendation, or favoring by the United States Government or any agency thereof. The views and opinions of authors expressed herein do not necessarily state or reflect those of the United States Government or any agency thereof.